HHS Public Access

Author manuscript

Res Vet Sci. Author manuscript; available in PMC 2017 August 01.

Published in final edited form as:

Res Vet Sci. 2016 August ; 107: 171–177. doi:10.1016/j.rvsc.2016.06.002.

Development of renal atrophy in murine 2 Kidney 1 Clip hypertension is strain independent

Sonu Kashyap[1], **Rajendra Boyilla**[1], **Paula J Zaia**[2], **Roba Ghossan**[3], **Karl A. Nath**[4], **Stephen C. Textor**[4], **Lilach O. Lerman**[4], and **Joseph P. Grande**[1,4]

[1]Department of Laboratory Medicine & Pathology, 179 11045-101 Boqueirao-Santos-SP Brazil

[2]Fundacao Lusiada-UNILUS Rua Oswaldo Cruz, 179 11045-101 Boqueirao-Santos-SP Brazil

[3]Saint Joseph University, Rue de Damas, Beirut, Lebanon

[4]Division of Nephrology & Hypertension Mayo Clinic, 200 First Street SW, Rochester, MN 55905 USA

Abstract

The murine 2-kidney 1-clip (2K1C) model has been used to identify mechanisms underlying chronic renal disease in human renovascular hypertension. Although this model recapitulates many of the features of human renovascular disease, strain specific variability in renal outcomes and animal-to-animal variation in the degree of arterial stenosis are well recognized limitations. In particular, the C57BLK/6 strain is considered to be resistant to chronic renal damage in other models. Our objectives were to determine strain dependent variations in renal disease progression and to identify parameters that predict renal atrophy in murine 2K1C hypertension. We used a 0.20 mm polytetrafluoroethylene cuff to establish RAS in 3 strains of mice C57BLK/6J (N=321), C57BLKS/J (N=177) and129Sv (N=156). The kidneys and hearts were harvested for histopathologic analysis after 3 days or after 1, 2, 4, 6, 7, 11 or 17 weeks. We performed multivariate analysis to define associations between blood pressure, heart and kidney weights, ratio of stenotic kidney/contralateral kidney (STK/CLK) weight, percent atrophy (% atrophy) and plasma renin content. The STK of all 3 strains showed minimal histopathologic alterations after 3 days, but later developed progressive interstitial fibrosis, tubular atrophy, and inflammation. The STK weight negatively correlated with maximum blood pressure and % atrophy, and positively correlated with STK/CLK ratio. RAS produces severe chronic renal injury in the STK of all murine strains studied, including C57BLK/6. Systolic blood pressure is negatively associated with STK weight, STK/CLK ratio and positively with atrophy and may be used to assess adequacy of vascular stenosis in this model.

Correspondence: Joseph P. Grande, M.D., Ph.D., Mayo Clinic, 200 First Street SW, Rochester MN 55905 USA., Tel: 1-507-284-9320, Fax: 1-507-266-1163, grande.joseph@mayo.edu.

Keywords

Renal artery stenosis; atrophy; mouse strains; hypertension

1. Introduction

Renal artery stenosis (RAS) is a common disease affecting human patients with other manifestations of atherosclerosis. Hemodynamically significant RAS can be detected in 6.8% of individuals over 65 and up to 40% in individuals with coronary or peripheral vascular disease (Hansen et al., 2002; Iglesias et al., 2000). RAS accounts for end stage renal disease in a substantial fraction of patients diagnosed with hypertensive nephrosclerosis (Freedman et al., 1995). Current medical therapies include revascularization through stenting and medical management with antihypertensive drugs (Textor, 2011). However, the recent Cardiovascular Outcomes in Renal Atherosclerotic Lesions (CORAL) trial showed that percutaneous transluminal renal angioplasty fails to improve renal function, renal or cardiovascular events, or patient survival (Cooper et al., 2014). Current medical therapy has limitations, as patients with atherosclerotic RAS have a death rate of 16% annually, mainly due to cardiovascular events (Kalra et al., 2010). The presence of RAS is an independent predictor for death independent of other conventional cardiovascular risk factors (Conlon et al., 1998; Edwards et al., 2005).

Based on these considerations, there is a clear need to define basic mechanisms leading to the development of chronic cardiovascular and renal disease in patients with RAS. We have developed a murine model of RAS, which involves placement of a polyfluorotetraethylene cuff on the right renal artery and recapitulates many of the findings observed in human RAS (Warner et al., 2012). A significant advantage of murine models of RAS stems from the availability of a wide variety of genetically modified animals that can be used to determine the mechanistic significance of various signaling pathways in the development of renal or cardiovascular disease. However, several potential limitations need to be addressed with murine models of RAS. It is recognized that there is considerable influence of genetic background on the development and progression of injury in various experimental models. For example, it is recognized that the C57BL/6J mouse is resistant to development of renal and cardiac fibrosis in various chronic injury models (Ma and Fogo, 2003; Walkin et al., 2013). For a given mouse strain, there may be experimental variability in the extent of atrophy achieved by RAS surgery. Finally, the interrelationships between the extent of atrophy and stenotic or contralateral kidney size, heart weights, or plasma angiotensin II content have not yet been fully established in a murine RAS model.

To address these issues, we performed a temporal analysis of the stenotic and contralateral kidney weights, blood pressure, and plasma angiotensin II content in 3 strains of mice. We find that the stenotic kidney of C57BLK/6J, C57BLKS/J, as well as 129Sv mice develops severe atrophy following RAS surgery. High systolic blood pressure, but not plasma angiotensin II content, strongly correlated with the development of atrophy in the stenotic kidney and compensatory enlargement of the contralateral kidney.

2. Materials and methods

2.1 Study animals

Mice were obtained from Jackson Laboratory (Bar Harbor, ME). We studied a total of 654 mice that underwent RAS or sham surgery. We characterized three different genetically unmodified strains of mice that are commonly employed to study renal disease progression in other experimental systems: C57BL/6J (N=205 RAS, N=116 sham), C57BLKS/J (N=129 RAS, N=48 sham) and 129Sv (N=112 RAS, N=44 sham) mice. Some of these animals served as controls in previously published studies (43 of 156 129Sv mice (Warner et al., 2012), 23 of 321 C57BL/6J mice (Wang et al., 2013), and 162 of 177 C57BLKS/J mice (Hartono et al., 2013, 2014; Kashyap et al., 2016). Additional mice, reported here, were used to support our ongoing studies to further characterize the 2 kidney 1 clip model and to define basic mechanisms of renal disease progression in this model. All animal protocols were approved by the Mayo Clinic Institutional Animal Care and Use Committee before performing the experiments.

2.2 2-Kidney-1-Clip murine model of renovascular hypertension

The 2-kidney-1 clip murine model of renovascular hypertension was established through placement of a a polytetrafluoroethylene cuff (0.5-mm length, 0.36-mm external diameter and 0.20 mm internal diameter) on the right renal artery (Warner et al., 2012). Sham surgery was performed with manipulation of the right renal artery without placement of the cuff. *In vivo* ultrasound imaging was performed using the Vevo 770 (VisualSonics, Toronto, Canada) in a subset of 50 mice as described previously (Warner et al., 2012). Mice were sacrificed at 3 days (N=58) and 1 (N=92), 2 (N=110), 4 (N=254), 6 (N=80), 7 (N=17) 11 (N=31) and 17 (N=12) weeks after RAS surgery for assessment of heart and kidney weights and histopathologic assessment of the STK.

2.3 Blood pressure measurements

Blood pressure measurements were performed on awake, unanesthetized mice using the tail cuff method (CODA System, Kent Scientific, Torrington, CT) before and after performing the RAS surgery and every week thereafter. The maximum systolic blood pressure reading during the study period was used for data analysis.

2.4 Biochemical analysis

Blood was collected via inferior vena cava at the end of study time point. The plasma was separated from blood and used for the renin content assay, measured as previously described (Hartono et al., 2013a).

2.5 Tissue harvesting and histology

At each time point, the animals were anesthetized and the kidneys were perfused with saline. Right and left kidneys and heart were excised and weighed. The kidneys were cut in half and a section of kidney containing the entire renal cortex and medulla was prepared. This section of Kidney was then fixed with 10% neutral buffered formalin and processed for histology using standard techniques. Histological sections (5 μm thick) were prepared and stained with

hematoxylin-eosin (H&E). The entire renal cortex was evaluated. Tubular atrophy, defined by a thickening of tubular basement membranes and a reduction in tubular diameter by over 50% compared to non-atrophic tubules, was qualitatively assessed as the percentage of renal cortex occupied by atrophic tubules relative to the total cortical surface area, and was expressed as a percentage (Racusen et al., 1999). Slides were read by an experienced renal pathologist (J.P.G.) in a blinded fashion, as previously described (Cheng et al., 2009; Warner et al., 2012).

2.6 Statistical analysis

Correlation analysis was performed using JMP 9.0.1. Parameters assessed included percent atrophy (%atrophy), right and left kidney weights, heart weight, the STK/CLK weight ratio, systolic blood pressure, and plasma renin content. Animals that had all the parameter values were included in the analysis. The correlation matrix was generated using Robust method. Principal component analysis was performed in JMP based on the correlation matrix.

ANOVA was performed for comparisons between groups using GraphPad Prism (GraphPad Software, La Jolla, CA).

3. Results

A representative photograph of a cuff placed on the right renal artery to establish renal artery stenosis is shown in figure 1a. An illustrative ultrasound image showing placement of the right renal artery cuff is shown in figure 1b. Representative repeated ultrasound measurements obtained at baseline, 2, 4, and 6 weeks shows a reduction in right kidney size with time following RAS induction (Fig. 1c).

A summary of stenotic kidney weights as a function of time following surgery for the 3 strains of mice is shown in table 1a. In all strains, the right (cuffed) kidney weight was reduced by 3 days after surgery (approximately −23% for C57BLKS/J, −27% for C57BL/6J, and −13% for 129Sv mice compared to respective sham; Table 1a). The decrease in kidney weights at 3 days did not reach statistical signicance for any of the strains. Stenotic kidney weights further decreased with time following surgery. Compared to sham mice, stenotic kidney weights were significantly reduced by 63% in C57BLKS/J mice, by 47% in C57BL/6J mice, and by 42% in 129Sv mice at 6 weeks following surgery (Table 1a). The contralateral kidney underwent compensatory enlargement in all mouse strains (Table 1b). A representative photomicrograph of stenotic and contralateral kidneys from C57BLK/6J mice subjected to RAS or sham procedures at 6 weeks following surgery is shown in figure 2a.

Results of histologic assessment of renal atrophy as a function of time following RAS or sham surgery are summarized in table 2. At 3 days following surgery, despite reduction in kidney weight, the stenotic kidneys showed minimal histopathologic alterations. Specifically, there were only isolated foci of tubular atrophy in C57BLKS/J and 129Sv mice, involving less than 1% of the cortical surface area (Table 2), with no evidence of acute tubular epithelial cell injury. No significant interstitial fibrosis or interstitial inflammation was observed at this time point.

Later time points were characterized by the development of progressive tubular atrophy (Table 2), affecting, on average, more than 40% of tubules in all strains studied. There were no significant differences in the mean % atrophy among the 3 murine strains studied (Table 2). A representative photomicrograph of renal cortex obtained from C57BLK/6 mice 6 weeks after being subjected to RAS or sham procedures is shown in figures 2b,c. The right (stenotic) kidney, following RAS, shows severe tubular atrophy, with interstitial inflammation and fibrosis, whereas the left (contralateral) kidney shows minimal histopathologic alterations, despite a 20% increase in weight. Both kidneys of mice subjected to sham surgery showed no significant histopathologic alterations (Fig. 2b,c).

The STK of all strains studied developed tubular atrophy to a similar extent, however there was some animal to animal variation in the extent of tubular atrophy that developed. Therefore, we sought to determine whether this variability could be predicted based on relationships between tubular atrophy and systolic blood pressure, plasma renin content (as measured by plasma angiotensin I production), heart weight, stenotic and contralateral kidney weight, and ratio of stenotic kidney/contralateral kidney weight (RK/CLK) in the 3 murine strains studied.

A summary of correlations for 129SV, C57BLK6/J, and C57BLKS mice are shown in tables 3a,b and c. There were strong negative correlations between STK weight, % atrophy [r= −0.8186 (129S), r=−0.9148 (C57BL6/J), r=−0.8400 (BLKS)], blood pressure [r=−0.4697 (129S), r=−0.4017 (C57BL6/J), r=−0.7727 (BLKS)] and positive correlation with STK/CLK ratio [r=0.8937 (129S), r=0.9647 (C57BL6/J), r=0.9790 (BLKS)]. Heart weight correlated with maximum blood pressure and CLK weight (Tables 3a, b), although the latter correlation was relatively weak for BLKS mice (Table 3c). Blood pressure was negatively correlated with STK weight and STK/CLK ratios in all strains. Plasma renin content did not correlate well with kidney weights (except with CLK weight in BLKS strain), heart weight, or blood pressure in any strain (Table 3a, b, c).

The overall relationships between kidney weights, STK/CLK ratio, blood pressure, heart weight and plasma renin content were similar among these three strains, therefore principal component analysis was performed on the aggregate data. A summary of overall correlations is provided in figure 3a. As expected, the STK weight was strongly correlated with the STK/CLK weight ratio (r=0.9380). Percent atrophy was strongly correlated with STK weight (r= −0.8604) and with STK/CLK ratio (r= −0.9160). Heart weight correlated best with CLK weight (r= 0.5645) and blood pressure (r=0.4123). Maximum blood pressure correlated best with STK weight (r=−0.4564) and STK/CLK ratio (r= −0.5206). On the other hand, plasma Angiotensin I production showed a modest positive correlation with heart weight (r=0.1552) and blood pressure (r=0.1800) and a modest negative correlation with % atrophy (r=− 0.1356).

Results of principal component analysis done on the correlation matrix (all mice strains data pooled together) are summarized in Figure 3b–d. Principal component 1 (PC1), which includes stenotic kidney weight, STK/CLK weight ratio and %atrophy accounted for 52.3% of the variance observed in the data. Principal component 2 (PC2), which included heart weight and angiotensin I for 18.4% of the variance. Principal component 3 consisted of CLK

wt and angiotensin I. The summary plots for the components are shown in figure 3b and c. figure 3b shows the individual observations according to time point and figure 3c illustrating the unit vectors in PC1 and PC2 space. A scatterplot 3D and summary of eigenvectors is shown in Figure 3d.

4. Discussion

Renal artery stenosis is a common clinical problem in human patients that is associated with considerable morbidity and mortality (de Mast and Beutler, 2009; Kalra et al., 2005; Textor, 2004). Recent studies have indicated that revascularization of the stenotic kidney fails to improve renal or patient outcomes (Cooper et al., 2014; Wheatley et al., 2009), although there is considerable controversy regarding this issue (White, 2010). These outcomes may be related to development of irreversible hypoxia, microvascular loss, and/or fibrosis in the STK so that up to 25% of revascularized patients develop progressive deterioration of renal function (Textor, 2003, 2004; Textor and Wilcox, 2001). Although current medical therapy clearly has a role in treating RAS, patients have a high death rate, mainly due to cardiovascular events (Kalra et al., 2010). Studies to define basic mechanisms of renal disease progression in RAS are clearly needed.

Since its initial description in the 1930's, the 2K1C model has been extensively used to mimic human renovascular hypertension (Goldblatt et al., 1934). The original model, which employed dogs, was one of accelerated hypertension, causing extensive damage to the contralateral kidney which was subjected to high blood pressure. In other species, including rats and mice, the animals do not develop malignant hypertension—the stenotic kidney develops progressive fibrosis and atrophy, whereas the contralateral kidney develops compensatory enlargement (Chade et al., 2003; Cheng et al., 2009; Eng et al., 1994; Gouvea et al., 2004; Thone-Reineke et al., 2003). Systemic activation of the renin-angiotensin-aldosterone system is essential for the early development of hypertension in this model (Basso and Terragno, 2001; DeForrest et al., 1982). The histopathologic alterations in murine RAS models (fibrosis and atrophy of the stenotic kidney and compensatory enlargement of the contralateral kidney in association with moderate hypertension) are similar to those observed in human RAS (Keddis et al., 2010).

In murine chronic renal injury models, it is well recognized that there are significant strain-specific differences in the extent of renal damage. In particular, the C57BLK/6 mouse is regarded to be resistant to development of chronic renal injury (Ma and Fogo, 2003; Walkin et al., 2013). However, no previous study has looked at strain-specific variability of renal outcomes in RAS. For this reason, we sought to determine whether there were any differences in the extent of STK chronic injury in 3 strains of mice widely employed in chronic renal injury models.

In all 3 strains, minimal histopathologic alterations were observed in the first 3 days following RAS surgery. This finding distinguishes the pattern of injury induced by cuff placement from that of ischemia-reperfusion injury (which produces tubular epithelial cell necrosis followed by repair) and indicates that the STK is able to compensate for the reduction in blood flow for a period of time after induction of RAS (Nath et al., 2011). After

this time point, the STK in all strains developed severe and progressive renal atrophy, characterized by tubular flattening and simplification, thickening of the tubular basement membranes, interstitial fibrosis, and interstitial inflammation. We did not discern any significant differences in the extent of tubular atrophy among the strains studied. In particular we found that the C57BLK/6 mouse, which is often considered to be resistant to development of chronic renal damage, developed severe renal atrophy several weeks after RAS surgery. This study provides the basis for future studies utilizing mice on the C57BLK/6 background to determine the mechanistic relevance of various signaling pathways on chronic renal disease progression.

Although the mean % atrophy in the STK was significantly increased at later time points following RAS surgery, in all 3 strains we noted animal-to-animal variability in the extent of atrophy, with many animals showing over 90% atrophy in the STK while others showed only 30–50%. We therefore sought to determine whether % atrophy was correlated with kidney or heart weights, blood pressure, or plasma angiotensin I production. In particular, we were interested in determining whether %atrophy correlated with maximum blood pressure or plasma angiotensin I production, which can be measured in live animals.

Maximum blood pressure correlated with heart weight, STK weight, and STK/CLK weight ratio. Of note, plasma angiotensin I production showed a negative correlation with % atrophy. In our previous studies, we found that angiotensin I production was transiently increased, peaking at approximately 2 weeks and returning to baseline levels after 6 weeks (Warner et al., 2012). A similar transient elevation of plasma angiotensin I production has been observed in human RAS (Garovic and Textor, 2005; Safian and Textor, 2001). It is likely that, as severe renal atrophy develops, the STK is less capable of activating the systemic renin-angiotensin system. In our study, STK with less atrophy appear to be more capable of increasing plasma renin production, accounting for the negative correlation between % atrophy and STK weight.

This is the first study to compare development of chronic renal damage in several distinct murine strains, yet was associated with several limitations. Our studies do not show how RAS interacts with other risk factors for cardiovascular disease—hyperlipidemia and diabetes in particular—to produce renal and vascular disease. Although patients with RAS are at high risk of developing cardiac morbidity and mortality, we have not yet studied the hearts in detail.

In summary, we have developed a murine model of RAS which recapitulates many of the features of human disease (Keddis et al., 2010) that may be employed in several distinct strains of mice currently used to study chronic renal disease in other systems. The use of a cuff to establish RAS produces a stable and reproducible stenosis without damaging the renal artery. This may facilitate future studies to determine the effects of cuff removal (to mimic stenting) on renal outcomes. Future mechanistic studies will determine the relevance of specific signaling pathways on the development of chronic renal damage through use of genetically modified (“knockout”) mice.

Acknowledgements

These studies were supported by NIH/NIAID R01 AI100911-01, DK73608 and DK104273.

References

Basso N, Terragno NA. History about the discovery of the renin-angiotensin system. Hypertension. 2001; 38:1246–1249. [PubMed: 11751697]

Chade AR, Rodriguez-Porcel M, Grande JP, Zhu XY, Sica V, Napoli C, Sawamura T, Textor SC, Lerman A, Lerman LO. Mechanisms of renal structural alterations in combined hypercholesterolemia and renal artery stenosis. Arteriosclerosis Thrombosis & Vascular Biology. 2003; 23:1295–1301.

Cheng J, Zhou W, Warner GM, Knudsen BE, Garovic VD, Gray CE, Lerman LO, Platt JL, Romero JC, Textor SC, Nath KA, Grande JP. Temporal analysis of signaling pathways activated in a murine model of 2-kidney, 1-clip hypertension. Am J Physiol Renal Physiol. 2009; 297:F1055–1068. [PubMed: 19625373]

Conlon PJ, Athirakul K, Kovalik E, Schwab SJ, Crowley J, Stack R, McCants CB Jr. Mark DB, Bashore TM, Albers F. Survival in renal vascular disease. J Am Soc Nephrol. 1998; 9:252–256. [PubMed: 9527401]

Cooper CJ, Murphy TP, Cutlip DE, Jamerson K, Henrich W, Reid DM, Cohen DJ, Matsumoto AH, Steffes M, Jaff MR, Prince MR, Lewis EF, Tuttle KR, Shapiro JI, Rundback JH, Massaro JM, D'Agostino RB, Dworkin LD. Stenting and Medical Therapy for Atherosclerotic Renal-Artery Stenosis. N Engl J Med. 2014; 370:13–22. [PubMed: 24245566]

de Mast Q, Beutler JJ. The prevalence of atherosclerotic renal artery stenosis in risk groups: a systematic literature review. J Hypertens. 2009; 27:1333–1340. [PubMed: 19365285]

DeForrest JM, Knappenberger RC, Antonaccio MJ, Ferrone RA, Creekmore JS. Angiotensin II is a necessary component for the development of hypertension in the two kidney, one clip rat. Am J Cardiol. 1982; 49:1515–1517. [PubMed: 6280481]

Edwards M, Craven T, Burke G, Dean R, Hansen K. Renovascular disease and the risk of adverse coronary events in the elderly: a prospective, population-based study. Archives of internal medicine. 2005; 165:207–213. [PubMed: 15668368]

Eng E, Veniant M, Floege J, Fingerle J, Alpers CE, Menard J, Clozel JP, Johnson RJ. Renal proliferative and phenotypic changes in rats with two-kidney, one-clip Goldblatt hypertension. Am J Hypertens. 1994; 7:177–185. [PubMed: 8179853]

Freedman BI, Iskandar SS, Appel RG. The link between hypertension and nephrosclerosis. American journal of kidney diseases : the official journal of the National Kidney Foundation. 1995; 25:207–221. [PubMed: 7847347]

Garovic VD, Textor SC. Renovascular hypertension and ischemic nephropathy. Circulation. 2005; 112:1362–1374. [PubMed: 16129817]

Goldblatt H, Lynch J, Hanzal R, Summerville W. Studies on experimental hypertension; I: The production of persistent elevation of systolic blood pressure by means of renal ischemia. J Exp Med. 1934; 59:347–379. [PubMed: 19870251]

Gouvea SA, Bissoli NS, Moysas MR, Cicilini MA, Pires JGP, Abreu GR. Activity of Angiotensin-Converting Enzyme After Treatment with L-Arginine in Renovascular Hypertension. Clinical & Experimental Hypertension. 2004; 26:569–579. [PubMed: 15554459]

Hansen KJ, Edwards MS, Craven TE, Cherr GS, Jackson SA, Appel RG, Burke GL, Dean RH. Prevalence of renovascular disease in the elderly: a population-based study. J Vasc Surg. 2002; 36:443–451. [PubMed: 12218965]

Hartono S, Knudsen B, Zubair A, Nath K, Textor S, Lerman L, Grande J. Redox Signaling Is an Early Event in the Pathogenesis of Renovascular Hypertension. Int J Mol Sci. 2013; 14:18640–18656. [PubMed: 24025423]

Hartono SP, Knudsen BE, Lerman LO, Textor SC, Grande JP. Combined effect of hyperfiltration and renin angiotensin system activation on development of chronic kidney disease in diabetic db/db mice. BMC Nephrol. 2014; 15:58. [PubMed: 24708836]

Iglesias JI, Hamburger RJ, Feldman L, Kaufman JS. The natural history of incidental renal artery stenosis in patients with aortoiliac vascular disease. Am J Med. 2000; 109:642–647. [PubMed: 11099684]

Kalra PA, Guo H, Gilbertson DT, Liu J, Chen SC, Ishani A, Collins AJ, Foley RN. Atherosclerotic renovascular disease in the United States. Kidney Int. 2010; 77:37–43. [PubMed: 19865075]

Kalra PA, Guo H, Kausz AT, Gilbertson DT, Liu J, Chen SC, Ishani A, Collins AJ, Foley RN. Atherosclerotic renovascular disease in United States patients aged 67 years or older: risk factors, revascularization, and prognosis. Kidney Int. 2005; 68:293–301. [PubMed: 15954920]

Kashyap S, Warner GM, Hartono SP, Boyilla R, Knudsen BE, Zubair AS, Lien K, Nath KA, Textor SC, Lerman LO, Grande JP. Blockade of CCR2 reduces macrophage influx and development of chronic renal damage in murine renovascular hypertension. Am J Physiol Renal physiol. 2016; 310:F372–384. [PubMed: 26661648]

Keddis MT, Garovic VD, Bailey KR, Wood CM, Raissian Y, Grande JP. Ischaemic nephropathy secondary to atherosclerotic renal artery stenosis: clinical and histopathological correlates. Nephrol Dial Transplant. 2010; 25:3615–3622. [PubMed: 20501460]

Ma L-J, Fogo AB. Model of robust induction of glomerulosclerosis in mice: importance of genetic background. Kidney International. 2003; 64:350–355. [PubMed: 12787428]

Nath KA, Croatt AJ, Warner GM, Grande JP. Genetic Deficiency of Smad3 Protects Against Murine Ischemic Acute Kidney Injury. Am J Physiol Renal Physiol. 2011; 301:F436–442. [PubMed: 21525133]

Racusen LC, Solez K, Colvin RB, Bonsib SM, Castro MC, Cavallo T, Croker BP, Demetris AJ, Drachenberg CB, Fogo AB, Furness P, Gaber LW, Gibson IW, Glotz D, Goldberg JC, Grande J, Halloran PF, Hansen HE, Hartley B, Hayry PJ, Hill CM, Hoffman EO, Hunsicker LG, Lindblad AS, Yamaguchi Y. The Banff 97 working classification of renal allograft pathology. Kidney Int. 1999; 55:713–723. [PubMed: 9987096]

Safian R, Textor S. Renal-artery stenosis. N Engl J Med. 2001; 344:431–442. [PubMed: 11172181]

Textor SC. Managing renal arterial disease and hypertension. Curr Opin Cardiol. 2003; 18:260–267. [PubMed: 12858123]

Textor SC. Ischemic nephropathy: where are we now? J Am Soc Nephrol. 2004; 15:1974–1982. [PubMed: 15284283]

Textor SC. Issues in renovascular disease and ischemic nephropathy: beyond ASTRAL. Curr Opin Nephrol Hypertens. 2011; 20:139–145. [PubMed: 21157335]

Textor SC, Wilcox CS. Renal artery stenosis: a common, treatable cause of renal failure? Annu Rev Med. 2001; 52:421–442. [PubMed: 11160787]

Thone-Reineke C, Olivier J, Godes M, Zart R, George I, Bauer C, Neumayer HH, Hocher B. Effects of angiotensin-converting enzyme inhibition and calcium channel blockade on cardiac apoptosis in rats with 2K1C (two-kidney/one-clip) renovascular hypertension. Clin Sci (Lond). 2003; 104:79–85. [PubMed: 12519090]

Walkin L, Herrick SE, Summers A, Brenchley PE, Hoff CM, Korstanje R, Margetts PJ. The role of mouse strain differences in the susceptibility to fibrosis: a systematic review. Fibrogenesis Tissue Repair. 2013; 6:18. [PubMed: 24294831]

Wang D, Warner GM, Yin P, Knudsen BE, Cheng J, Butters KA, Lien KR, Gray CE, Garovic VD, Lerman LO, Textor SC, Nath KA, Simari RD, Grande JP. Inhibition of p38 MAPK attenuates renal atrophy and fibrosis in a murine renal artery stenosis model. Am J Physiol Renal Physiol. 2013; 304:F938–947. [PubMed: 23364805]

Warner GM, Cheng J, Knudsen BE, Gray CE, Deibel A, Juskewitch JE, Lerman LO, Textor SC, Nath KA, Grande JP. Genetic deficiency of Smad3 protects the kidneys from atrophy and interstitial fibrosis in 2K1C hypertension. Am J Physiol Renal Physiol. 2012; 302:F1455–1464. [PubMed: 22378822]

Wheatley K, Ives N, Gray R, Kalra PA, Moss JG, Baigent C, Carr S, Chalmers N, Eadington D, Hamilton G, Lipkin G, Nicholson A, Scoble J. Revascularization versus medical therapy for renal-artery stenosis. N Engl J Med. 2009; 361:1953–1962. [PubMed: 19907042]

White CJ. Kiss My Astral: One seriously flawed study of renal stenting after another. Catheterization and Cardiovascular Interventions. 2010; 75:305–307. [PubMed: 20095015]

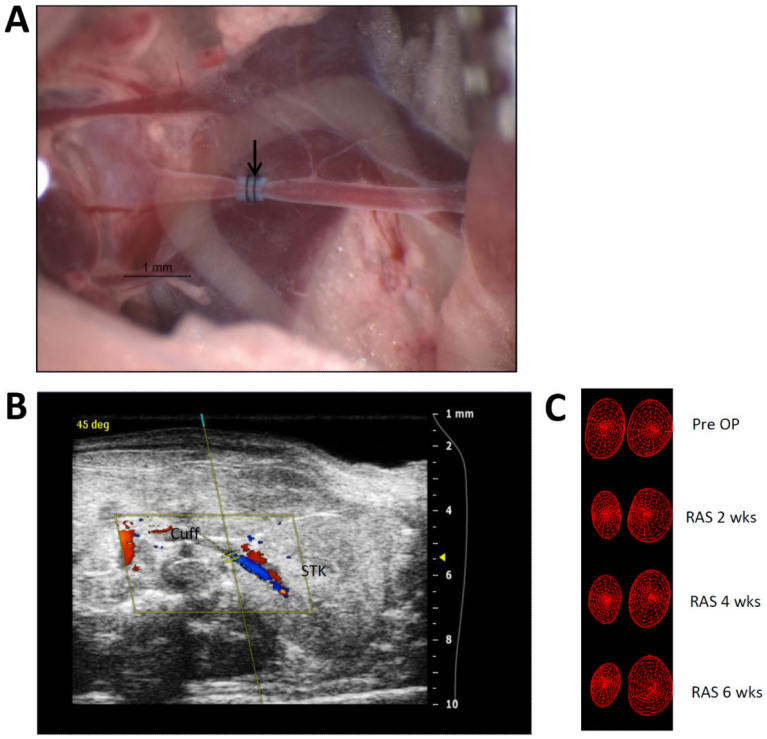

Fig. 1.

A. Representative image of the right artery showing the position of cuff with arrow head. **B.** Ultrasound image showing the cuffed kidney. **C.** 3D wireframe reconstruction from ultrasound showing the reduction in the size of cuffed kidney and increase in contralateral kidney over time following RAS.

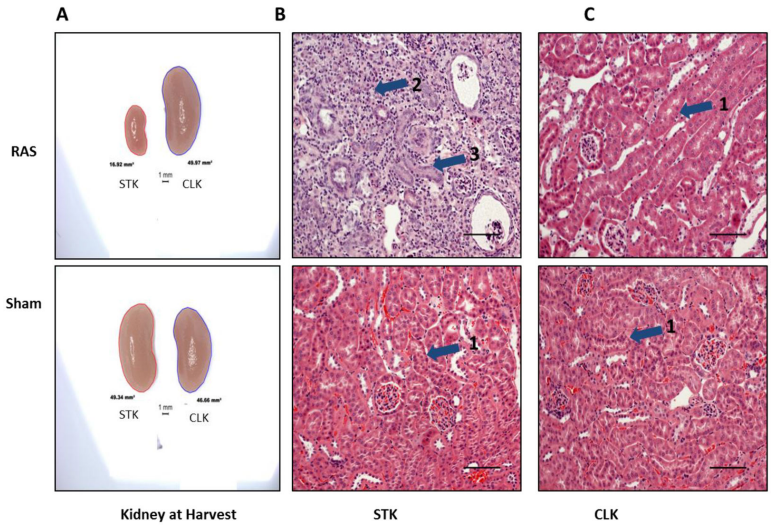

Fig. 2.

A. Representative images of the kidneys of Sham and RAS at harvest. Right cuffed kidney in RAS showing the reduction in the size of right kidney and increase in CLK in RAS. **B and C.** Representative images of right and contralateral kidney respectively with RAS or sham stained with H&E stain at 200× magnification. Histologic appearance of the sham kidneys (B, C lower) and the contralateral kidney of a mouse with RAS (C, upper) is normal, with back-to-back tubules with abundant eosinophilic (pink staining) cytoplasm and thin, delicate tubular basement membranes (pointed by arrow head 1). The right (stenotic) kidney of a RAS mouse shows severe and generalized tubular atrophy, characterized by a marked reduction in tubular diameter, thickening of tubular basement membranes, and influx of chronic inflammatory cells (pointed by arrow head 2). A relatively presereved tubule is pointed by arrow head 3.

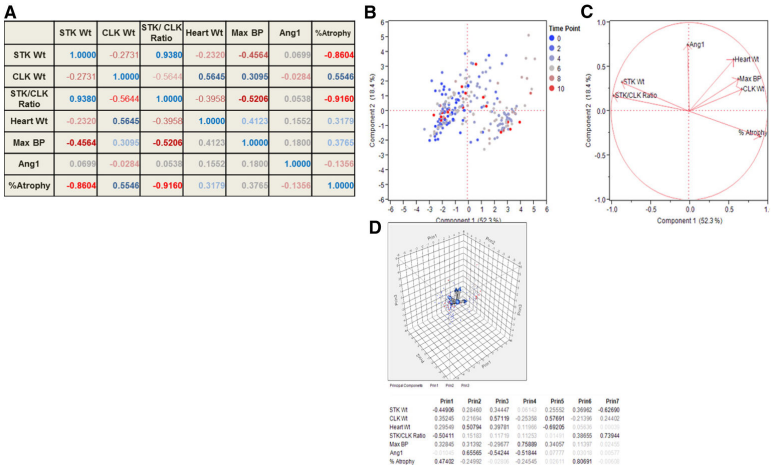

	STK Wt	CLK Wt	STK/ CLK Ratio	Heart Wt	Max BP	Ang1	%Atrophy
STK Wt	1.0000	-0.2731	0.9380	-0.2328	-0.4564	0.0699	-0.8604
CLK Wt	-0.2731	1.0000	-0.5644	0.5645	0.3095	-0.0284	0.5546
STK/CLK Ratio	0.9380	-0.5644	1.0000	-0.3958	-0.5206	0.0538	-0.9160
Heart Wt	-0.2328	0.5645	-0.3958	1.0000	0.4123	0.1662	0.3179
Max BP	-0.4564	0.3095	-0.5206	0.4123	1.0000	0.1800	0.3765
Ang1	0.0699	-0.0284	0.0538	0.1662	0.1800	1.0000	-0.1366
%Atrophy	-0.8604	0.5546	-0.9160	0.3179	0.3765	-0.1366	1.0000

Fig. 3.

A. Showing the correlation matrix between variables in 2K1C RAS model in all strain of mice pooled together. Cells are color coded by magnitude and sign of their correlation values. **B.** Bi-plot showing individual observations plotted in two-dimensional PC1 and PC2 space, color coded by time points following surgery. **C.** Unit vectors in PC1-PC2 space corresponding to measured variables. **D.** Scatterplot 3D in PC1-PC2-PC3 space and eigenvectors for the measured variables.

Table 1

A. Mean±SEM stenotic kidney weight (mg) from three different mice stains following RAS or sham surgery as function of time. **B.** Mean±SEM contralateral kidney weight (mg) from three different mice stains following RAS or sham surgery as function of time.

A.

	3D		1wk		2wk		4wk		6wk		7wk		11WK		17WK	
Strain	**RAS**	**Sham**	**RAS**	**Sham**	**RAS**	**Sham**	**RAS**	**Sham**	**RAS**	**Sham**	**RAS**	**Sham**	**RAS**	**Sham**	**RAS**	**Sham**
BLKS/J	156±5.4 (N=14)	203±5.2 N=11	116±7.3 N=16	223±3.3 N=10	97±6.4 N=22	202±8.6 N=11	98±5.0 N=60	192±13.0 N=7	74.4±13.0 N=9	200±5.5 N=5	N/A	N/A	N/A	N/A	44±10.2 N=8	253±8.5 N=4
BL/6J	129±6.3 N=10	177±15.2 N=8	111±4.0 N=26	151±4.3 N=24	90±11.2 N=8	150±5.5 N=12	80±3.8 N=128	164±3.1 N=59	80±11.2 N=12	150±7.5 N=3	N/A	N/A	49±8.8 N=21	177±9.2 N=10	N/A	N/A
129S	157±7.7 N=12	180±0.0 N=3	132±7.7 N=10	157±5.3 N=6	107±5.5 N=39	156±7.6 N=18	N/A	N/A	92±8.8 N=37	158±9.9 N=14	71±12.8 N=14	177±3.3 N=3	N/A	N/A	N/A	N/A

B.

	3D		1wk		2wk		4wk		6wk		7wk		11WK		17WK	
Strain	**RAS**	**Sham**	**RAS**	**Sham**	**RAS**	**Sham**	**RAS**	**Sham**	**RAS**	**Sham**	**RAS**	**Sham**	**RAS**	**Sham**	**RAS**	**Sham**
BLKS/J	186±8.2 (N=14)	181±5.1 N=11	184±4.5 N=16	194±3.4 N=10	196±3.9 N=22	183±5.5 N=11	220±4.8 N=60	160±6.4 N=7	200±9.4 N=9	194±6.8 N=5	N/A	N/A	N/A	N/A	320±8.5 N=8	238±6.3 N=4
BL/6J	142±4.4 N=10	166±12 N=8	156±4.5 N=26	150±4.7 N=24	157±7.5 N=8	150±4.6 N=12	181±2.8 N=128	154±2.5 N=59	209±12.8 N=12	149±3.3 N=3	N/A	N/A	203±8.7 N=21	171±6.2 N=10	N/A	N/A
129S	183±6.4 N=12	177±8.8 N=3	178±3.9 N=10	150±8.1 N=6	159±5.1 N=39	152±8.2 N=18	N/A	N/A	177±5.3 N=37	152±9.9 N=14	199±7.6 N=14	157±8.8 N=3	N/A	N/A	N/A	N/A

Table 2

Mean±SEM % atrophy of stenotic kidney of three different mice strains following RAS surgery as function of time.

Strain	3D	1wk	2wk	4wk	6wk	7wk	11wk	17wk
BLKS/J	0.1±0.1 N=14	46.9±5.1 N=16	50.6±7.4 N=22	56.6± 5.2 N=60	62.4±14.3 N=9	N/A	N/A	71.8±12.8 N=4
BL/6J	1±0.3 N=7	26.6±7.2 N=26	56.1±13.4 N=8	51.6±3.7 N=129	47.3±11.4 N=10	N/A	63.8±8.6 N=18	N/A
129S	0.2+0.2 N=12	22±10.5 N=10	33.9±6.8 N=39	N/A	43.6±7.2 N=37	59.5±10.2 N=14	N/A	N/A

Table 3

A. Showing the correlation matrix between variables in 2K1C RAS model in 129S mouse strain. **B.** Showing the correlation matrix between variables in 2K1C RAS model in C57BL/6J mouse strain. **C.** Showing the correlation matrix between variables in 2K1C RAS model in C57BLKS/J mouse strain. Cells are color coded by magnitude and sign of their correlation values.

A		**STK Wt**	**CLK Wt**	**STK/ CLK Ratio**	**Heart Wt**	**Max BP**	**Ang1**	**%Atrophy**
	STK Wt	1.0000	−0.0150	0.8937	−0.1622	−0.4697	−0.0538	−0.8186
	CLK Wt	−0.0150	1.0000	−0.4402	0.7096	0.3029	−0.0941	0.4452
	STK/CLK Ratio	0.8937	−0.4402	1.0000	−0.4393	−0.5808	−0.0012	−0.9163
	Heart Wt	−0.1622	0.7096	−0.4393	1.0000	0.3462	0.0849	0.3752
	Max BP	−0.4697	0.3029	−0.5808	0.3462	1.0000	0.1552	0.4076
	Ang1	−0.0538	−0.0941	−0.0012	0.0849	0.1552	1.0000	−0.1271
	%Atrophy	−0.8186	0.4452	−0.9163	0.3752	0.4076	−0.1271	1.0000
B		**STK Wt**	**CLK Wt**	**STK/ CLK Ratio**	**Heart Wt**	**Man BP**	**Ang1**	**%Atrophy**
	STK Wt	1.0000	−0.5417	0.9647	−0.2532	−0.4017	0.1770	−0.9148
	CLK Wt	−0.5417	1.0000	−0.7061	0.4972	0.2822	−0.2004	0.624
	STK/CLK Ratio	0.9647	−0.7061	1.0000	−0.3664	−0.4503	0.1689	−0.9105
	Heart Wt	−0.2532	0.4972	−0.3664	1.0000	0.4668	0.1854	0.2571
	Max BP	−0.4017	0.2822	−0.4503	0.4868	1.0000	0.1561	0.3024
	Ang1	0.1770	−0.2004	0.1689	0.1854	0.1561	1.0000	−0.3500
	%Atrophy	−0.9148	0.6240	−0.9105	0.2571	0.3024	−0.3500	1.0000
C		**STK Wt**	**CLK Wt**	**STK/ CLK Ratio**	**Heart Wt**	**Max BP**	**Ang1**	**%Atrophy**
	STK Wt	1.0000	−0.1556	0.9790	−0.2375	−0.7727	−0.0633	−0.8400
	CLK Wt	−0.1556	1.0000	−0.3378	0.1600	−0.0364	−0.5687	0.4051
	STK/CLK Ratio	0.9790	−0.3378	1.0000	−0.2702	−0.7352	0.0235	−0.8741
	Heart Wt	−0.2375	0.1600	−0.2702	1.0000	0.3806	0.2017	0.2326
	Max BP	−0.7727	−0.0364	−0.7352	0.3806	1.0000	0.2569	0.5589
	Ang1	−0.0633	−0.5687	0.0235	0.2017	0.2569	1.0000	−0.0602
	%Atrophy	−0.8400	0.4051	−0.8741	0.2326	0.5589	−0.0602	1.0000

STK Wt = stenotic kidney weight, CLK Wt= contralateral kidney weight, BP = blood pressure, Ang1= angiotensin I.